

## Dilepton production in proton-proton and quasifree proton-neutron reactions at 1.25 GeV

R. Shyam<sup>1,2</sup> and U. Mosel<sup>1</sup>

<sup>1</sup>*Institut für Theoretische Physik, Universität Giessen, D-35392 Giessen, Germany*

<sup>2</sup>*Saha Institute of Nuclear Physics, Kolkata 700064, India*

(Received 30 September 2010; published 15 December 2010)

We investigate the  $pp \rightarrow ppe^+e^-$  and quasifree  $pn \rightarrow pne^+e^-$  reactions within an effective Lagrangian model at a laboratory kinetic energy of 1.25 GeV for which experimental data have recently been reported by the HADES Collaboration. The model uses a meson-exchange approximation to describe the initial nucleon-nucleon ( $NN$ ) scattering. Contributions to the reaction amplitudes are included from the  $NN$  bremsstrahlung as well as from the excitation, propagation, and radiative decay of the  $\Delta(1230)$  isobar state. It is found that the HADES data on the  $e^+e^-$  invariant mass distribution in the  $pp \rightarrow ppe^+e^-$  reaction are excellently reproduced by our model where the  $\Delta$  isobar term dominates the spectrum. In the case of the quasifree  $pn \rightarrow pne^+e^-$  reaction, a strong sensitivity to the pion electromagnetic form factor is observed which helps to bring the calculated cross sections closer to the data in the higher dilepton mass region.

DOI: [10.1103/PhysRevC.82.062201](https://doi.org/10.1103/PhysRevC.82.062201)

PACS number(s): 25.75.Dw, 13.30.Ce, 12.40.Yx

Dileptons ( $e^+e^-$ ) provide a valuable tool to investigate the properties of the strongly interacting matter at high temperature and density formed in the relativistic and ultrarelativistic nuclear collisions because after their production they travel to the detectors almost undisturbed by the surrounding baryonic matter. A recurring feature of the dilepton spectra measured in such collisions at low (DLS and HADES Collaborations [1,2]), intermediate super proton synchrotron (SPS [3]), and high (PHENIX Collaboration [4]) energies has been the significant enhancement observed in the intermediate dilepton mass region over the contributions from the electromagnetic decays of hadrons and long-lived mesons. While the major part of the excess yield seen at the SPS energies is attributed to the leptonic decay of the  $\rho$  meson (formed in the  $\pi^+\pi^-$  annihilation process) with strongly modified spectral functions in dense and hot hadronic matter [5], at relativistic heavy ion collider (RHIC) energies it is believed to be more due to the strong thermal contribution from the partonic phase (see, e.g., Ref. [6]).

At lower beam energies (1–2 GeV/nucleon), various transport models [7–10] have been unable to explain the DLS data, which must be attributed to some inherent problems in the theory as the new measurements of the HADES Collaboration at these beam energies have confirmed the old DLS data [11]. Unlike the situation at high beam energies, the causes of this discrepancy—for the light systems at least—are unlikely to be related to the in-medium effects. The insufficiently known cross sections for the dilepton production in elementary proton-proton ( $pp$ ) and proton-neutron ( $pn$ ) collisions are an important reason behind this. Indeed, in a recent transport model calculation [12] it has been shown that if the input  $pn$  bremsstrahlung cross sections (which are calculated within the soft-photon approximation model [13]), are scaled up in an *ad hoc* manner by factors of 3–4, the observed dilepton yields of both DLS and HADES experiments at beam energies of 1–2 GeV/nucleon can be reproduced.

However, the microscopic models of dilepton production in elementary  $NN$  reactions differ in their predictions of the  $pn$  bremsstrahlung cross section. While the calculations

performed within the effective Lagrangian models of Refs. [14–17] do not support the larger  $pn$  bremsstrahlung yields, those of the model of Refs. [18] favor the enhanced cross sections implemented in Ref. [12]. Therefore, to provide a reliable constraint for the dilepton yields in elementary reactions, the HADES Collaboration has very recently performed measurements for the dilepton production in not only the  $pp$  reaction but also in the quasifree  $pn$  reaction at 1.25 GeV beam kinetic energy [19]. The latter was measured by colliding a proton target with a deuteron beam of kinetic energy 1.25 GeV/nucleon and by detecting fast spectator protons from the deuteron breakup in a dedicated forward direction. In Ref. [19] the data on both  $pp$  and quasifree  $pn$  reactions were compared with the predictions of the model of Ref. [18] where it was noted that the calculations fail to describe the data for both reactions. While in the  $pp$  case the dilepton yields were overestimated in the entire range of the dilepton invariant mass ( $M$ ), those of the quasifree  $pn$  reaction were overestimated (underestimated) at lower (higher) regions of  $M$ .

The aim of this Rapid Communication is to investigate the dilepton production in  $pp$  and quasifree  $pn$  reactions at a beam energy of 1.25 GeV within the effective Lagrangian model (ELM) of Refs. [14,16,17]. In order to compare our calculations with the HADES dilepton yields, we have also considered the following additional features: (i) For the quasifree  $pn$  reaction the available energy in the center-of-mass (c.m.) system has been smeared to include the momentum distribution of the neutron in the deuteron using the Argonne V18 [20] deuteron wave function: as a consequence, the  $dp$  reaction results in a smeared  $pn$  (quasifree) reaction where the available c.m. energies could be in excess of the threshold for the  $\eta$ -meson production (see, e.g., Ref. [21]); (ii) because of this we have included the  $\eta$  Dalitz decay cross sections in the total theoretical yields for the  $pn$  reaction; and (iii) the contributions from the production and dileptonic decay of the subthreshold  $\rho^0$  meson via the baryonic resonance  $N^*(1520)$  have been included for both  $pp$  and quasifree  $pn$  reactions.

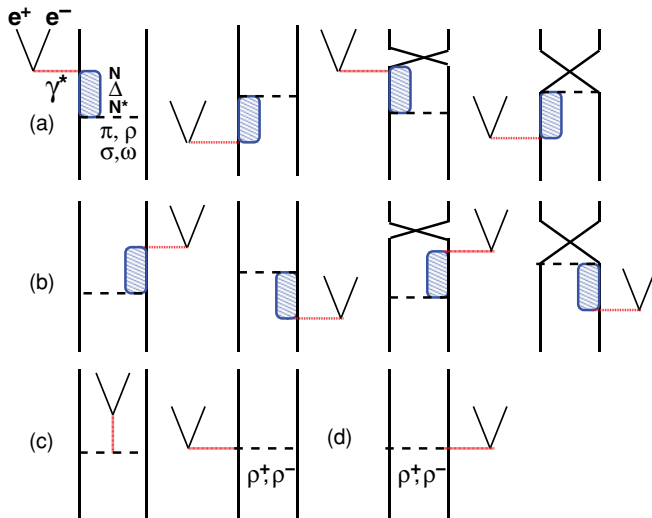


FIG. 1. (Color online) Graphical representation of our model to describe  $e^+e^-$  production in  $pp$  and  $pn$  collisions. Diagrams (a) and (b) represent the  $e^+e^-$  emission from an external nucleon line. (c)  $e^+e^-$  emission from an internal charged meson line for the  $pn$  reaction. (d) Diagrams representing processes where  $e^+e^-$  is emitted directly from the charged meson-nucleon-nucleon-photon vertices.

The Feynman diagrams [corresponding to both postemission and preemission (direct and exchange) processes] contributing to the dilepton production in the ELM are shown in Fig. 1. In the case of the charged pion exchange (which occurs for the  $pn$  reaction) the internal meson line can also lead to dilepton emission [Fig. 1(c)]. The initial interaction between two incoming nucleons is modeled by an effective Lagrangian which is based on the exchange of the  $\pi$ ,  $\rho$ ,  $\omega$ , and  $\sigma$  mesons. The coupling constants at the nucleon-nucleon-meson vertices are determined by directly fitting the  $T$  matrices of the  $NN$  scattering in the relevant energy region [14]. These parameters are quite robust and have been used in successful descriptions of the  $NN \rightarrow NN\pi$  [22],  $pp \rightarrow p\Lambda K^+$ ,  $pp \rightarrow p\Sigma^0 K^+$  [23,24], and  $NN \rightarrow NN\eta$  [25] reactions.

The dilepton production proceeds via excitation, propagation, and radiative decay of the intermediate nucleon or resonance states at either of the two colliding nucleon vertices [Figs. 1(a) and 1(b)]. The nucleon intermediate states give rise to the  $NN$  bremsstrahlung contribution. In calculations of various amplitudes we have used the same effective Lagrangians (and the corresponding parameters) for all of the hadronic and electromagnetic vertices as those given in Refs. [16,17]. We recall that for the  $NN\pi$  vertex we have employed a pseudoscalar (PS) coupling where no derivative term of the pion field is involved. Therefore, no extra term (corresponding to a contact or the seagull diagram) appears in the model at the  $NN\pi$  vertex when the electromagnetic coupling is included via the substitution  $\partial^\mu \rightarrow \partial^\mu - imA^\mu$  (where  $m$  is +1, 0, and  $-1$  for positive, neutral, and negative pions, respectively). However, at the  $NN\rho$  vertices such terms are always present as the corresponding coupling also involves the derivative of the meson field [26–28]. In any case,  $\rho$ -meson exchange terms contribute less than 5% to the

total bremsstrahlung cross sections [29]. Thus, our calculations performed with a PS  $NN\pi$  coupling are almost free from the gauge-invariance-related ambiguities, which could be associated with the contact terms (see, e.g., Ref. [30]).

A note of caution should, however, be added here. With a PS  $NN\pi$  coupling the role of negative energy states may be overestimated, whereas these are quite suppressed with the corresponding pseudovector (PV) interaction. Nevertheless, only the bremsstrahlung dilepton production amplitudes are expected to be affected by the PS-PV coupling choice. Because both  $pp \rightarrow ppe^+e^-$  and  $pn \rightarrow pne^+e^-$  reactions are dominated by the delta isobar contributions at a beam energy of 1.25 GeV (as is shown in the following), our overall conclusions are not affected by the choice of the coupling at the  $NN\pi$  vertex. In any case, the nucleon-antinucleon vertex may be considerably suppressed compared to the  $NN$  vertex in the presence of timelike form factors [31].

As a beam kinetic energy of 1.25 GeV is below the threshold of the  $NN\eta$  channel (1.258 GeV), there is no contribution to the  $pp \rightarrow ppe^+e^-$  cross sections from the  $\eta$  Dalitz decay process. However, as explained earlier, this can contribute to the quasifree  $pn$  reactions. The  $\pi^0$  Dalitz decay contributions must be taken into account as they dominate the cross sections at the lower ends of the dilepton invariant mass distributions in both reactions.

The  $\eta$  Dalitz decay is treated as a two-step process—the  $\eta$ -meson production by reactions  $p + n \rightarrow p + n + \eta$  and  $p + n \rightarrow d + \eta$ , followed by the  $\eta$ -meson Dalitz decay. The total cross sections for the  $\eta$ -meson production reactions have been taken from Ref. [25], where a good description of the corresponding experimental data [32] is obtained. The  $\eta$  Dalitz decay to  $\gamma e^+e^-$  is calculated by using expressions given in Ref. [33]. A similar procedure is applied for the  $\pi^0$  case where the production cross sections have been taken from Ref. [22], while for its Dalitz decay the formulas of Ref. [33] have been utilized.

In calculations of dilepton yields from the production and decay of the subthreshold  $\rho^0$  meson via the baryonic resonances, we consider only the  $N^*(1520)$  resonance—other higher-lying resonances are expected to contribute negligibly at the beam energy considered in this Rapid Communication [34]. We suppose this reaction to proceed as a  $NN \rightarrow RN \rightarrow \rho^0 NN \rightarrow e^+e^- NN$  process (where  $R$  represents a resonance), which leads to the following factorization of the cross section:

$$\frac{d\sigma(s, M)^{NN \rightarrow NN e^+ e^-}}{dM} = \frac{d\sigma(s, M)^{NN \rightarrow \rho^0 NN}}{dM} \frac{\Gamma_{\rho^0 \rightarrow e^+ e^-}(M)}{\Gamma_{\rho}^{\text{tot}}(M)},$$

where  $s$  is the square of the invariant mass associated with the incident channel. In Eq. (1) the first term on the right-hand side represents the differential cross section for the  $\rho^0$ -meson production in  $NN$  collisions, which is calculated by following the procedure described in Refs. [35,36] using the same parameters as those given in Ref. [36]. The second term is the branching ratio for the  $\rho^0 \rightarrow e^+e^-$  decay.  $\Gamma_{\rho^0 \rightarrow e^+e^-}$  is the decay width of the  $\rho^0$  meson to the dilepton channel, which is calculated within a strict vector meson dominance model as in Ref. [34].  $\Gamma_{\rho}^{\text{tot}}$  is the total  $\rho$ -meson width, which is

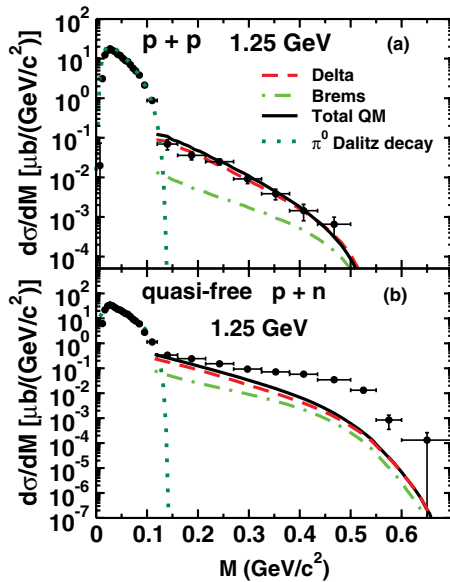


FIG. 2. (Color online) (a) The invariant mass distribution of the dileptons produced in the  $pp \rightarrow ppe^+e^-$  reaction at a beam energy of 1.25 GeV. The maximum allowed value of  $M$  is 0.545 GeV for this beam energy. (b) The same for the quasifree  $pn \rightarrow pne^+e^-$  reaction at the same incident energy. The Fermi smearing as discussed in the text has been applied to all the theoretical calculations shown in Fig. 2(b). Experimental data are from Ref. [19].

given by [37]

$$\Gamma_{\rho}^{\text{tot}}(M) = \Gamma_{\rho^0 \rightarrow \pi\pi} \frac{r_C^2 k^3}{M(1 + r_C^2 k^2)}, \quad (1)$$

where  $k^2 = M^2/4 - m_{\pi}^2$ . The parameter  $r_C$  represents an interaction radius, which is taken to be 2 fm and  $\Gamma_{\rho^0 \rightarrow \pi\pi} = 0.150$  GeV. Equation (2) represents the partial width for the  $\rho$ -meson decay to the  $2\pi$  channel only, which has a branching ratio of nearly 100%. In our calculations, however, we have also added to it the width  $\Gamma_{\rho^0 \rightarrow e^+e^-}$ .

In Fig. 2(a), we compare the calculated and measured dilepton invariant mass ( $M$ ) distributions for the  $pp \rightarrow ppe^+e^-$  reaction at a beam kinetic energy of 1.25 GeV. We recall that for this reaction, only diagrams 1(a) and 1(b) contribute. The theoretical cross sections have been folded with the appropriate detector acceptances provided to us by the HADES Collaboration [38]. We see that the total cross section (solid line) (obtained by the coherent summation of  $NN$  bremsstrahlung and  $\Delta$  isobar amplitudes, which will be referred to as QM) for this reaction is dominated by the  $\Delta$  isobar terms (dashed line). The  $NN$  bremsstrahlung contributions (dashed-dotted line) are smaller by almost an order of magnitude for lower values of  $M$  and by factors of 3–5 at higher  $M$ . The region of  $M < 0.15$  GeV/ $c^2$  is dominated by the  $\pi^0$  Dalitz decay cross sections.

It clear that our QM cross sections for the  $pp \rightarrow ppe^+e^-$  reaction are in excellent agreement with the HADES data for  $M > 0.15$  GeV/ $c^2$ . In contrast to this, the model of Ref. [18] overestimates the data everywhere in this region (see Fig. 1 of Ref. [19]). A similar observation was also made in comparisons with the DLS  $pp$  dilepton data at 1.04 GeV

beam energy in Ref. [17]. Since this reaction is dominated by the  $\Delta$  contributions, the larger  $\Delta$  cross sections of Ref. [18] as compared to those of our model are the most likely reason for the differences seen in the predications of the two models.

In Fig. 2(b), we show the same results for the quasifree  $pn \rightarrow pne^+e^-$  reaction at 1.25 GeV beam kinetic energy. Because of the Fermi smearing, the tails of various contributions extend to  $M$  values larger than those of the  $pp$  reaction, which is in agreement with the data. However, the shape of the  $pn$  spectra differs significantly in several ways from that of the  $pp$  case in the region of  $M$  beyond that dominated by the  $\pi^0$  Dalitz decay process. First, the  $NN$  bremsstrahlung contribution is now relatively larger although the  $\Delta$  isobar term still dominates the total cross section. Second, the QM cross sections significantly underpredict the HADES quasifree  $pn$  data for  $M > 0.20$  GeV/ $c^2$ , which is in sharp contrast to the  $pp$  case. The difference between theory and the data varies from factors of 2–3 at the lower mass values to more than an order of magnitude for  $M$  around 0.5 GeV/ $c^2$ . It is important to understand this discrepancy between calculations and the data for the quasifree  $pn \rightarrow pne^+e^-$  reaction because the dilepton excess in the intermediate mass range of  $0.15 < M < 0.60$  GeV/ $c^2$  observed in  $C + C$  collisions at 1 and 2 GeV/nucleon can be explained by a superposition of experimental elementary  $pp$  and  $pn$  reactions with in-medium effects being almost negligible [19].

In none of the results shown so far (in Figs. 2(a) and 2(b), as well as in Refs. [16,17]), were electromagnetic form factors considered at any of the vertices. However, in the earlier work reported in Ref. [14] it was shown that the hadronic electromagnetic form factors have a significant influence on the dilepton spectra. Therefore, we now include the pion electromagnetic form factor (PEFF) [ $F_{\pi}(M^2)$ ] at the charged internal meson line [Fig. 1(c)]. In the present exploratory study we use the same form factors at both the pion and the nucleon vertices in order to preserve gauge invariance [14,28]. We have used two parametrizations for  $F_{\pi}(M^2)$ . The first one (to be referred to as FF1) is written as

$$F_{\pi}(M^2) = \frac{m_{\rho}^2}{m_{\rho}^2 - M^2 - im_{\rho}\Gamma_{\rho}(M^2)},$$

where  $m_{\rho}$  is the  $\rho$ -meson mass and  $\Gamma_{\rho}$  is the width for  $\rho \rightarrow \pi\pi$  decay. The assumption inherent in FF1 is that the photon couples to the pion only via the  $\rho^0$  meson. It reproduces the main features of the pion EFF both in time- and spacelike regions (see Ref. [39]). The other, to be referred to as FF2, described extensively in Ref. [40], is

$$F_{\pi}(M^2) = \frac{0.4}{1 - M^2/\lambda^2} + \frac{0.6}{1 - M^2/2m_{\rho}^2} \frac{m_{\rho}^2}{m_{\rho}^2 - M^2 - im_{\rho}\Gamma_{\rho}(M^2)},$$

where  $\lambda^2 = 1.9$  GeV $^2$ . The width  $\Gamma_{\rho}(M^2)$  appearing in both FF1 and FF2 has been calculated by following the expressions given in Ref. [40]. FF2 is derived from the assumption that the photon couples about 50% directly to the intrinsic quark

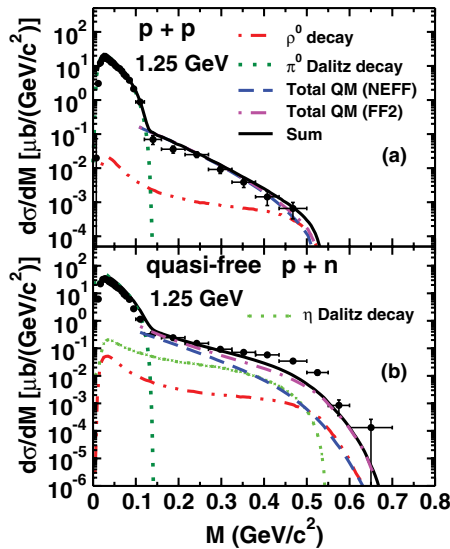


FIG. 3. (Color online) (a) and (b) The same reactions as in Figs. 2(a) and 2(b) but with electromagnetic form factors included at pion and nucleon vertices. Also shown are the contributions of meson Dalitz decays and subthreshold  $\rho^0$  decay processes. Total QM cross sections obtained with (FF2) and without (NEFF) electromagnetic form factors are shown by dashed and dashed-dotted lines, respectively. The simple sum of the meson Dalitz decays,  $\rho^0$  decay, and full quantum mechanical (with FF2 form factors) cross sections are shown by the solid line. The data are taken from Ref. [19].

structure of the pion and the remaining 50% indirectly through the  $\rho^0$  meson. FF2 provides a better description of the PEFF in the timelike region. The imaginary parts of both FF1 and FF2 are proportional to two-pion phase space—below two-pion production thresholds, both FF1 and FF2 are real. It should be stressed here that we have put both form factors on the mass shell. Given the high virtuality of the internal pions, the form factors should be functions of both pion momentum and the momentum transfer. However, knowledge of the off-shell pion form factor is still scanty—the recent extraction of the PEFF from the JLab electroproduction experiments essentially provides information about the on-shell pion form factors only (see, e.g., Ref. [41]). Therefore, we use the on-shell PEFF in these calculations with a caveat that the off-shell PEFF could be larger than the on-shell one [42].

In Fig. 3(a), we show the effect of the PEFF and the contributions of the  $\pi^0$  Dalitz decay and subthreshold  $\rho^0$  decay process for the  $pp \rightarrow ppe^+e^-$  reaction. We note that, for this case, the introduction of the electromagnetic form factors (which are assumed to be the same for both the proton and pion vertices) makes hardly any difference to the results obtained without them. The effect of the FF2 type of PEFF is barely observed only at the extreme end of the spectrum. Results obtained with the FF1 form factor are not shown here—they are even closer to the no-PEFF results. Furthermore, the subthreshold  $\rho$  decay cross sections too are of some relevance only in the extreme tail region.

In Fig. 3(b), we show the total QM cross sections obtained without (NEFF) and with (FF2) the electromagnetic form

factor of FF2 type for the quasifree  $pn \rightarrow pne^+e^-$  reaction [where Fig. 1(c) also contributes] at a beam energy of 1.25 GeV. We have not shown explicitly the cross sections obtained with the FF1 type of PEFF in order not to overcrowd the figure—they lie between the NEFF and FF2 results. The larger cross sections obtained with FF2 form factors as compared to those with FF1 form factors can be traced back to the fact that in the timelike region the former is significantly larger than the latter [39,40]. We note that with the FF2 type of PEFF, the QM cross sections are significantly enhanced for  $M > 0.3$  GeV/ $c^2$  and are larger than  $\eta$  and  $\rho^0$  decay contributions by almost an order of magnitude at larger values of  $M$ . The  $\eta$  Dalitz decay contributions drop off significantly for  $M$  beyond 0.50 GeV/ $c^2$  due to phase-space restrictions. In this region the  $\rho^0$  decay cross sections become relatively stronger. It is seen that the simple sum of the QM (with FF2) and the meson decay cross sections is now able to reproduce the data for  $M$  up to  $\simeq 0.4$  GeV/ $c^2$  and for  $M > 0.55$  GeV/ $c^2$ . It should, however, be stressed that there is a danger of double counting by explicitly including  $\rho$ -meson production and decay terms together with the form factor FF2, which implicitly includes a  $\rho$ -meson bump. However, because the contributions of the explicit  $\rho^0$ -meson production process are relatively quite small as compared to that of the form factor FF2, this problem may not be too serious.

We remark that the final-state interaction (FSI) effects ( $pn$  and  $pp$ ) estimated within the Watson-Migdal method increase the magnitudes of the cross sections with increasing  $M$  value. However, even at the extreme kinematical limits the FSI-related enhancements in the cross sections are not more than 15%–20% for those reactions at 1.25 GeV. This result is in agreement with those of Ref. [18]. Furthermore, the deuteronlike final states have also not been considered because the HADES measurements have ruled out such states in their data.

In summary, we extended our effective Lagrangian model for dilepton production in nucleon-nucleon collisions by including the pion electromagnetic form factors at the internal meson line in a way that still preserves gauge invariance and employed it to describe the new data of the HADES Collaboration for these reactions.

For the quasifree  $pn \rightarrow pne^+e^-$  reaction, the inclusion of the electromagnetic form factors significantly enhances the cross sections for dilepton masses larger than 0.3 GeV/ $c^2$ . Thus, the dilepton production data in elementary proton-neutron reactions are shown to be very sensitive to the pion electromagnetic form factors. Although this effect was already noted in the early work of Ref. [14], it could not be affirmed at that time because of the absence of data on the elementary  $pn$  process. We find that the simple sum of the  $\pi^0$  Dalitz decay and the ELM cross sections is able to describe the experimental invariant mass distribution of the dileptons everywhere except for the three points lying between 0.40 and 0.55 GeV/ $c^2$ . The  $\eta$  Dalitz and  $\rho^0$  decay processes are of only minor consequence.

For the  $pp \rightarrow ppe^+e^-$  reaction, the ELM, which remains almost unaffected by the electromagnetic form factors, provides on its own a good description of the data for

dilepton invariant masses  $>0.15 \text{ GeV}/c^2$ . This is in marked contrast to the results shown in Ref. [19] where the model of Ref. [18] is found to grossly overestimate the data in this region. The simple sum of ELM cross sections and those of the meson decay processes provide an excellent description of the data in the entire region of the dilepton invariant mass.

The authors are thankful to Ingo Fröhlich and Tetyana Galatyuk for their help in implementing the acceptances of the HADES detector in our theoretical calculations. This work is supported by the Federal Ministry of Education and Research (BMBF). One of the authors (R.S.) acknowledges support from the Helmholtz International Center for FAIR under the LOEWE program.

- 
- [1] R. J. Porter *et al.*, *Phys. Rev. Lett.* **79**, 1229 (1997).  
 [2] G. Agakichiev *et al.*, *Phys. Rev. Lett.* **98**, 052302 (2007); *Eur. Phys. J. A* **41**, 243 (2009).  
 [3] G. Agakichiev *et al.*, *Eur. Phys. J. C* **41**, 475 (2005); D. Adamova *et al.*, *Phys. Lett. B* **666**, 425 (2008); *Phys. Rev. Lett.* **91**, 042301 (2003); R. Arnaldi *et al.*, *ibid.* **96**, 162302 (2006).  
 [4] S. Afanasiev *et al.*, arXiv:0706.3034 [nucl-ex].  
 [5] R. Rapp, *Nucl. Phys. A* **782**, 275c (2007); H. van Hees and R. Rapp, *Phys. Rev. Lett.* **97**, 102301 (2006); J. Ruppert, C. Gale, T. Renk, P. Lichard, and J. I. Kapusta, *ibid.* **100**, 162301 (2008).  
 [6] A. Drees, *Nucl. Phys. A* **830**, 435c (2009).  
 [7] E. L. Bratkovskaya, W. Cassing, R. Rapp, and J. Wambach, *Nucl. Phys. A* **634**, 168 (1998).  
 [8] C. Ernst, S. A. Bass, M. Belkacem, H. Stöcker, and W. Greiner, *Phys. Rev. C* **58**, 447 (1998).  
 [9] R. Rapp and J. Wambach, *Adv. Nucl. Phys.* **25**, 1 (2000).  
 [10] K. Shekhter, C. Fuchs, A. Faessler, M. Krivoruchenko, and B. Martemyanov, *Phys. Rev. C* **68**, 014904 (2003).  
 [11] G. Agakishiev *et al.*, *Phys. Lett. B* **663**, 43 (2008).  
 [12] E. L. Bratkovskaya and W. Cassing, *Nucl. Phys. A* **807**, 214 (2008).  
 [13] C. Gale and J. Kapusta, *Phys. Rev. C* **35**, 2107 (1987); **40**, 2397 (1989).  
 [14] M. Schäfer, H. C. Dönges, A. Engel, and U. Mosel, *Nucl. Phys. A* **575**, 429 (1994).  
 [15] F. de Jong and U. Mosel, *Phys. Lett. B* **379**, 45 (1996).  
 [16] R. Shyam and U. Mosel, *Phys. Rev. C* **67**, 065202 (2003).  
 [17] R. Shyam and U. Mosel, *Phys. Rev. C* **79**, 035203 (2009).  
 [18] L. P. Kaptari and B. Kämpfer, *Nucl. Phys. A* **764**, 338 (2006); *Phys. Rev. C* **80**, 064003 (2009).  
 [19] G. Agakishiev *et al.* (HADES Collaboration), *Phys. Lett. B* **690**, 118 (2010).  
 [20] R. B. Wiringa, V. G. J. Stoks, and R. Schiavilla, *Phys. Rev. C* **51**, 38 (1995).  
 [21] I. Froehlich *et al.*, arXiv:0909.5373 [nucl-ex].  
 [22] R. Shyam and U. Mosel, *Phys. Lett. B* **426**, 1 (1998).  
 [23] R. Shyam, *Phys. Rev. C* **60**, 055213 (1999).  
 [24] R. Shyam, G. Penner, and U. Mosel, *Phys. Rev. C* **63**, 022202(R) (2001).  
 [25] R. Shyam, *Phys. Rev. C* **75**, 055201 (2007).  
 [26] D. O. Riska, *Prog. Part. Nucl. Phys.* **11**, 199 (1984).  
 [27] K. Haglin, J. Kapusta, and C. Gale, *Phys. Lett. B* **224**, 433 (1989).  
 [28] K. L. Haglin, *Ann. Phys. (NY)* **212**, 84 (1993).  
 [29] R. Shyam and U. Mosel, *Pramana-J. Phys.* **75**, 185 (2010).  
 [30] A. Usov and O. Scholten, *Phys. Rev. C* **72**, 025205 (2005).  
 [31] S. J. Brodsky, *Comments Nucl. Part. Phys.* **12**, 213 (1984).  
 [32] H. Calén *et al.*, *Phys. Rev. C* **58**, 2667 (1998); *Phys. Rev. Lett.* **80**, 2069 (1998).  
 [33] L. G. Landsberg, *Phys. Rep.* **128**, 301 (1985).  
 [34] E. L. Bratkovskaya, W. Cassing, M. Effenberger, and U. Mosel, *Nucl. Phys. A* **653**, 301 (1999).  
 [35] B. Friman and H. J. Pirner, *Nucl. Phys. A* **617**, 496 (1997).  
 [36] W. Peters, M. Post, H. Lenske, S. Leupold, and U. Mosel, *Nucl. Phys. A* **632**, 109 (1998).  
 [37] D. M. Manley and E. M. Saleski, *Phys. Rev. D* **45**, 4002 (1992); M. Effenberger, Ph.D. thesis, Justus-Liebig-Universitaet Giessen, 1999 (unpublished).  
 [38] I. Fröhlich (private communication).  
 [39] T. Ericson and W. Weise, *Pions and Nuclei* (Clarendon, Oxford, 1988).  
 [40] G. E. Brown, M. Rho, and W. Weise, *Nucl. Phys. A* **454**, 669 (1986).  
 [41] V. Tadevosyan *et al.*, *Phys. Rev. C* **75**, 055205 (2007).  
 [42] S. J. Brodsky, in *At the Frontier of Particle Physics*, edited by M. Shifman (World Scientific, Singapore, 2001).